~~CONFIDENTIAL~~

Copy
RM H55H25

NACA

RESEARCH MEMORANDUM

FLIGHT MEASUREMENTS OF THE VERTICAL-TAIL LOADS ON THE CONVAIR XF-92A DELTA-WING AIRPLANE

By Clinton T. Johnson

High-Speed Flight Station
Edwards, Calif.

NATIONAL ADVISORY COMMITTEE
FOR AERONAUTICS

WASHINGTON

October 27, 1955

~~CONFIDENTIAL~~

NATIONAL ADVISORY COMMITTEE FOR AERONAUTICS

RESEARCH MEMORANDUM

FLIGHT MEASUREMENTS OF THE VERTICAL-TAIL LOADS ON THE CONVAIR XF-92A DELTA-WING AIRPLANE

By Clinton T. Johnson

SUMMARY

The aerodynamic loads acting over the vertical tail were determined from steady and maneuvering flight during the investigation of the lateral stability and control characteristics of the Convair XF-92A airplane. The results presented in this paper were obtained from rudder pulses and gradually increasing sideslips over the Mach number range from 0.50 to 0.87 at altitudes between 30,000 feet and 20,000 feet.

The vertical-tail panel bending-moment and normal-force characteristics are essentially linear with increasing sideslip angle both in rudder-fixed and trimmed maneuvers. A comparison of the bending-moment and normal-force parameters derived from rudder-fixed oscillations and the corresponding parameters derived from gradual manuevers indicates similar trends with Mach number. The effect of rudder deflection is to reduce the slope of the vertical-tail normal-force-coefficient variation with sideslip angle and to move the lateral location of the center of pressure of the additional air load inboard about 5 percent of the span of the vertical-tail panel.

The vertical-tail bending-moment and normal-force coefficients resulting from rudder deflections are essentially constant below a Mach number of 0.80 with an apparent tendency for both parameters to increase at the higher Mach numbers tested.

INTRODUCTION

As part of the cooperative Air Force—Navy—NACA flight research program, the delta-wing Convair XF-92A airplane was utilized for flight investigations at the NACA High-Speed Flight Station at Edwards, Calif.

The primary purpose of these flight investigations was to evaluate the handling qualities, lift and drag characteristics, aerodynamic loads

and load distribution, control surface loads, and buffeting characteristics. During the test program the flight envelope was extended to the maximum lift and Mach number attainable. Results of several of these investigations are reported in references 1 to 4.

Vertical-tail loads were measured by strain-gage methods during these flight investigations to provide full-scale flight loads information on a low-aspect-ratio triangular vertical-tail configuration such as used on the XF-92A airplane. This paper presents the results of the measurements of vertical-tail loads during rudder pulses, rudder-fixed oscillations, and gradually increasing sideslips at level-flight lift coefficients at altitudes between 30,000 feet and 20,000 feet up to a Mach number of 0.87.

SYMBOLS

b_{vt} span of vertical-tail panel outboard of gage station, in.

$C_{b_{vt}}$ vertical-tail panel bending-moment coefficient, $\frac{M_{b_{vt}}}{qS_{vt}b_{vt}}$

$C_{b_{\delta_r}}$ variation of vertical-tail panel bending-moment coefficient with rudder deflection, per deg, $\frac{\partial C_{b_{vt}}}{\partial \delta_r}$

$C_{N_{vt}}$ vertical-tail panel normal-force coefficient, $\frac{L_{vt}}{qS_{vt}}$

C_{N_β} variation of vertical-tail panel normal-force coefficient with angle of sideslip for zero rudder deflection, per deg, $\frac{\partial C_{N_{vt}}}{\partial \beta}$

$C_{N_{\delta_r}}$ variation of vertical-tail panel normal-force coefficient with rudder deflection, per deg, $\frac{\partial C_{N_{vt}}}{\partial \delta_r}$

c_{vt} chord at any section, in.

$\bar{c}_{vt}$ mean aerodynamic chord of vertical-tail panel, in.

$$\frac{\int_0^{b_{vt}} c_{vt}^2 \, dy}{\int_0^{b_{vt}} c_{vt} \, dy}$$

$\frac{dC_{N_{vt}}}{d\beta}$ slope of normal-force-coefficient variation with sideslip angle for trimmed sideslip, per deg

cp_A lateral location of the center of pressure of the additional air load of the vertical-tail panel, percent b_{vt}

h_p pressure altitude, ft

L_{vt} vertical-tail panel aerodynamic load (positive load to the left), lb

M free-stream Mach number

$M_{b_{vt}}$ vertical-tail panel bending moment about vertical-tail strain-gage station (positive conterclockwise when viewed from the rear), in-lb

p rolling velocity, radians/sec

q free-stream dynamic pressure, lb/ft^2

r yawing velocity, radians/sec

S_{vt} area of vertical-tail panel outboard of strain-gage station, ft^2

t time, sec

y spanwise distance along vertical tail, in.

β indicated sideslip angle, deg

δ_r rudder position, deg

AIRPLANE

The Convair XF-92A is a semitailless, delta-wing airplane with a 60° leading-edge sweepback of the wing and vertical stabilizer. The wing and vertical tail have a streamwise thickness ratio of 6.5 percent. The elevons and rudder are full-span, constant-chord surfaces with small, unshielded horn balances near the tips. Control surfaces are actuated by a 100-percent hydraulically boosted system. The airplane has no dive brakes and no leading- or trailing-edge flaps or slats.

A three-view drawing of the airplane is shown in figure 1 and photographs are shown in figure 2. Table I lists the physical characteristics of the airplane.

INSTRUMENTATION AND ACCURACY

The Convair XF-92A airplane was equipped with standard NACA recording instruments for recording the following quantities pertinent to this investigation:

Airspeed
Altitude
Normal and transverse acceleration
Rolling angular velocity and acceleration
Yawing angular velocity and acceleration
Control positions
Angle of attack and angle of sideslip

A multichannel oscillograph was used for recording strain-gage outputs and a common timer was used to correlate all instruments.

Strain gages were installed on the vertical tail spars at the vertical tail root (approximately 4 inches outboard of the vertical tail-fuselage juncture as shown in fig. 1) to measure shear and bending moment. The data presented in this paper have been corrected for the inertia of the vertical tail and are the aerodynamic loads acting over the vertical-tail surface.

The accuracy of the measured loads was determined from the results of a static calibration and an evaluation of the strain-gage responses in flight. The estimated error in shear and bending moment is ±300 pounds and ±8,000 inch-pounds, respectively. Estimated accuracies of other pertinent recorded quantities are:

Mach number, M	±0.01
r, radians/sec	±0.02
p, radians/sec	±0.10
β, deg	±0.25
δ_r, deg	±0.20

TESTS

The flight tests were conducted in the clean configuration at level-flight lift coefficients. Vertical-tail loads were measured during abrupt rudder pulses, rudder-fixed oscillations with the aileron held fixed, and gradually increasing sideslips using ailerons to hold constant heading over the Mach number range from 0.50 to 0.87 at altitudes from 30,000 feet to 20,000 feet. Reynolds number, based on the wing mean aerodynamic chord, varied between 25×10^6 and 50×10^6 for this series of tests. The center of gravity varied between 27.1 and 28.2 percent of the wing mean aerodynamic chord.

RESULTS AND DISCUSSION

Time histories of representative rudder pulses at several Mach numbers are presented in figure 3 showing the rudder input, the resulting vertical-tail loads, and airplane motions. The initial portion of the maneuvers shows the rudder deflection and the corresponding change in vertical-tail bending-moment and normal-force coefficients before the airplane responds to the control input. This portion of the maneuver is indicated by the solid lines in figure 3 occuring near t = 1.0 second. Since rudder deflection, vertical-tail bending-moment, and normal-force coefficient were the only variables during this portion of the maneuver, it was possible to determine the vertical-tail-load parameters $C_{b_{\delta_r}}$ and $C_{N_{\delta_r}}$. It may be noted that small changes in sideslip angle (less than 0.1°) did occur during the time the rudder was being deflected. However, the error in the values of $C_{N_{\delta_r}}$ and $C_{b_{\delta_r}}$, caused by a change of 0.1° in sideslip angle, was estimated to be less than 20 percent based on the values of normal-force-curve slope and the center of pressure of the additional air load ascertained from this investigation.

The Mach number variation of the vertical-tail-load parameters $C_{b_{\delta_r}}$ and $C_{N_{\delta_r}}$ determined from rudder pulses is shown in figure 4. The parameters $C_{b_{\delta_r}}$ and $C_{N_{\delta_r}}$ are relatively constant below a Mach

number of 0.80 at levels of about -0.009 per degree and -0.017 per degree, respectively. At the higher Mach numbers a slight increase in both parameters is apparent.

The solid lines in the latter portion of the maneuvers beginning near t = 2.0 seconds of figure 3 show the airplane oscillations after the rudder has been returned to neutral. From this portion of the maneuver the vertical-tail normal-force coefficient $C_{N_{vt}}$ was plotted with respect to sideslip angle β and appeared to have a linear variation with sideslip over the range of sideslip angles investigated. Therefore, slopes of these data were taken to determine the parameter C_{N_β}. (Normal-force increments caused by rolling and yawing velocities were evaluated and were found to be negligible). Typical plots used to determine C_{N_β} and the variation of C_{N_β} with Mach number are shown in figure 5. The vertical-tail-load parameter C_{N_β} is constant at a level near 0.035 per degree to a Mach number of 0.70, then increases gradually to a value near 0.045 per degree at M = 0.87.

The center of pressure of the additional air load cp_A for the rudder-fixed oscillations was determined by taking slopes of the variation of bending-moment coefficient $C_{b_{vt}}$ with $C_{N_{vt}}$. Typical plots used to determine cp_A and the variation of cp_A with Mach number are shown in figure 6. The lateral location of the center of pressure of the additional air load is located at approximately 45 percent of the span of the vertical-tail panel over the Mach number range from 0.50 to 0.87.

The vertical-tail loads measured during gradually increasing sideslips over the Mach number range from 0.50 to 0.85 are shown in figures 7 to 9. It may be noted that sideslips were performed using sufficient aileron to hold a constant heading. Aileron angles varied from approximately 4° at low speeds to 2° at high speeds. The parameters determined from these maneuvers are compared with the parameters obtained from the rudder-undeflected maneuvers to illustrate the effect of rudder deflection on the vertical-tail loads.

Figure 7 shows the variation of the vertical-tail normal-force coefficient $C_{N_{vt}}$ with sideslip angle and the corresponding rudder required to sideslip for several maneuvers over the Mach number range. The data of figure 7 are shown in figure 8 as the variation with Mach number of the slopes of the vertical-tail normal-force coefficient

resulting from trimmed sideslips $\frac{dC_{N_{vt}}}{d\beta}$ and the ratio of rudder deflection to sideslip angle $\frac{d\delta_r}{d\beta}$. The parameter $\frac{dC_{N_{vt}}}{d\beta}$ for trimmed sideslip has a value of approximately 0.028 per degree to a Mach number of 0.75, then increases gradually to 0.032 per degree at M = 0.85.

The curve of C_{N_β} determined from rudder-fixed maneuvers (fig. 5) is also shown on figure 8. The difference in level between the curves of C_{N_β} and $\frac{dC_{N_{vt}}}{d\beta}$ illustrates the change in normal-force-curve slope attributable to rudder deflection and is relatively constant over the Mach number range. The reduction in rudder-fixed C_{N_β} is approximately 20 percent.

It is interesting to note that the variation of $\frac{dC_{N_{vt}}}{d\beta}$ with Mach number can be derived using $C_{N_{\delta_r}}$ from figure 4, $\frac{d\delta_r}{d\beta}$ from figure 8, and C_{N_β} from figure 5, since $\frac{dC_{N_{vt}}}{d\beta} = C_{N_{\delta_r}} \times \frac{d\delta_r}{d\beta} + C_{N_\beta}$. This method was used to calculate the variation of vertical-tail normal-force coefficient with sideslip angle and agreed very closely with the measured data and slopes of figure 7.

The variation of bending-moment coefficient $C_{b_{vt}}$ with normal-force coefficient $C_{N_{vt}}$ and the resultant cp_A for the trimmed sideslips is shown in figure 9. The center of pressure of the additional air load for the trimmed sideslips is located at approximately 40 percent b_{vt} over the Mach number range from 0.50 to 0.85. A comparison of the centers of pressure of the additional air load determined from rudder-fixed and trimmed sideslip maneuvers indicates that rudder deflection moves the cp_A inboard approximately 5 percent of b_{vt} over the Mach number range tested.

CONCLUSIONS

Flight measurements of the vertical-tail loads on the Convair XF-92A airplane over the Mach number range from 0.50 to 0.87 during

rudder pulses and gradually increasing sideslips have indicated the following conclusions:

1. The vertical-tail panel characteristics are essentially linear throughout the angle of sideslip and Mach number range tested.

2. The vertical-tail load parameters derived from the rudder-fixed oscillations and steady sideslip maneuvers display similar trends with Mach number, with differences in level indicating the effect of rudder deflection on the vertical-tail loads. The predominant effect of rudder deflection on the vertical-tail loads is to reduce the normal-force curve slope C_{N_β} approximately 20 percent and to move the center of pressure of the additional air load cp_A inboard approximately 5 percent of the span of the vertical-tail panel.

3. The vertical-tail bending and normal-force coefficients resulting from rudder deflections $C_{b_{\delta_r}}$ and $C_{N_{\delta_r}}$ are essentially constant below a Mach number of 0.80 with both parameters indicating a tendency to increase at the higher Mach numbers tested.

High-Speed Flight Station,
National Advisory Committee for Aeronautics,
Edwards, Calif., August 15, 1955.

REFERENCES

1. Sisk, Thomas R., and Muhleman. Duane O.: Lateral Stability and Control Characteristics of the Convair XF-92A Delta-Wing Airplane as Measured in Flight. NACA RM H55A17, 1955.

2. Sisk, Thomas R., and Muhleman Duane O.: Longitudinal Stability Characteristics in Maneuvering Flight of the Convair XF-92A Delta-Wing Airplane Including the Effects of Wing Fences. NACA RM H54J27, 1955.

3. Kuhl, Albert E., and Johnson, Clinton T.: Flight Measurements of Wing Loads on the Convair XF-92A Delta-Wing Airplane. NACA RM H55D12, 1955.

4. Johnson, Clinton T., and Kuhl, Albert E.: Flight Measurements of Elevon Hinge Moments on the XF-92A Delta-Wing Airplane. NACA RM H54J25a, 1955.

TABLE I. - PHYSICAL CHARACTERISTICS OF THE XF-92A AIRPLANE

Wing:	
Area, sq ft	425
Span, ft	31.33
Airfoil section	NACA $65_{(06)}$-006.5
Mean aerodynamic chord, ft	18.09
Aspect ratio	2.31
Root chord, ft	27.13
Tip chord	0
Taper ratio	0
Sweepback (leading edge), deg	60
Incidence, deg	0
Dihedral (chord plane), deg	0
Elevons:	
Area (total, both, rearward of hinge line), sq ft	76.19
Horn balance area (total, both, elevons forward of hinge line), sq ft	1.4
Span (one elevon), ft	13.35
Chord (rearward of hinge line, constant except at tip), ft	3.05
Movement, deg	
Elevator:	
Up	15
Down	5
Aileron, total	10
Operation	Hydraulic
Vertical tail:	
Area, above fuselage center line, sq ft	126.5
Area, exposed, sq ft	75.35
Height, above fuselage center line, ft	11.70
Height, exposed, ft	8.96
Airfoil section	NACA $65_{(06)}$-006.5
Mean aerodynamic chord (area above fuselage center line), in.	167.45
Mean aerodynamic chord of exposed area, in.	129.40
Aspect ratio of area above fuselage center line	1.085
Aspect ratio of exposed area	1.065
Root chord at fuselage center line, in.	251.15
Root chord of exposed area, in.	194
Tip chord	0
Taper ratio	0
Sweepback (leading edge), deg	60
Vertical tail panel outboard of gage station:	
Area, sq ft	70
Span, in.	103.7
Mean aerodynamic chord, in.	124.7
Fuselage station of leading edge of mean aerodynamic chord, in.	324.08
Tail length to panel quarter chord at gross-weight center of gravity, in.	68.14
Aspect ratio	1.065
Root chord, in.	187.07
Rudder:	
Area, sq ft	15.53
Span, ft	9.22
Travel, deg	±8.5
Operation	Hydraulic
Fuselage:	
Length, ft	42.80
Maximum diameter, ft	5.58
Power plant:	
Engine	Allison J33-A-29 with afterburner
Rating:	
Static thrust at sea level, lb	5,600
Static thrust at sea level with afterburner, lb	7,500
Weight:	
Gross weight (560 gal fuel), lb	15,560
Empty weight, lb	11,808
Center-of-gravity locations:	
Gross weight (560 gal fuel), percent M.A.C.	25.5
Empty weight, percent M.A.C.	29.2
Inertia characteristics:	
Moment of inertia in yaw, (average value through 0° to 8° angle of attack at average gross weight), slug-ft^2	38,400
Moment of inertia in roll, (average value through 0° to 8° angle of attack at average gross weight), slug-ft^2	6,000
Inclination of principal axis of inertia, (estimated), deg	1.0

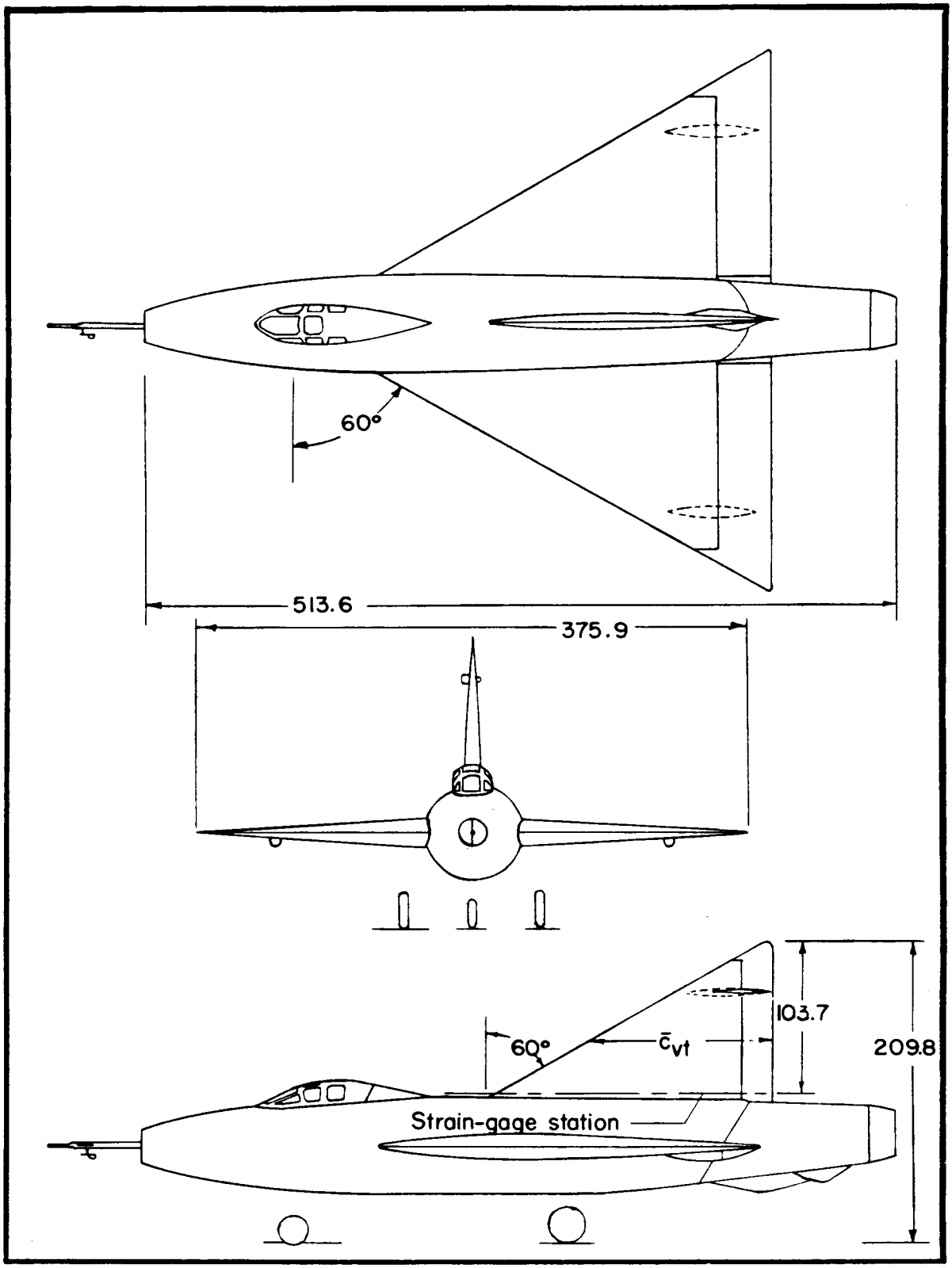

Figure 1.- A three-view drawing of the XF-92A airplane. All dimensions are in inches.

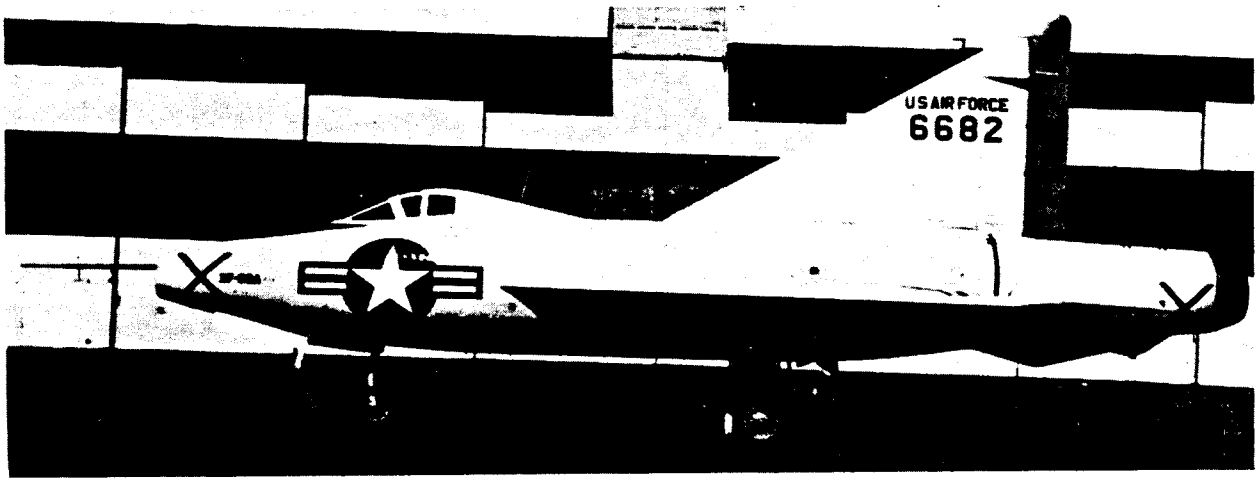

(a) Left side view.

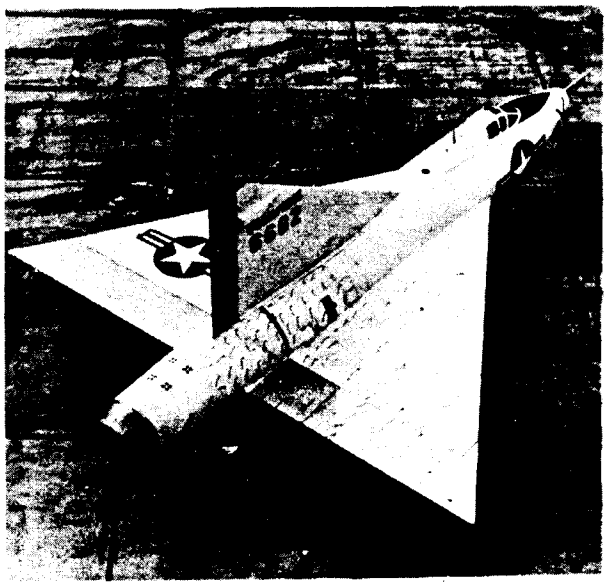

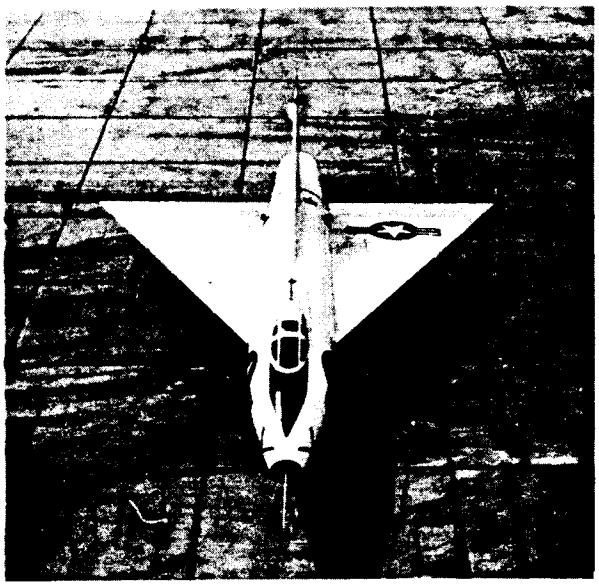

L-89388

(b) Three quarter rear view. (c) Overhead front view.

Figure 2.- Photographs of XF-92A research airplane.

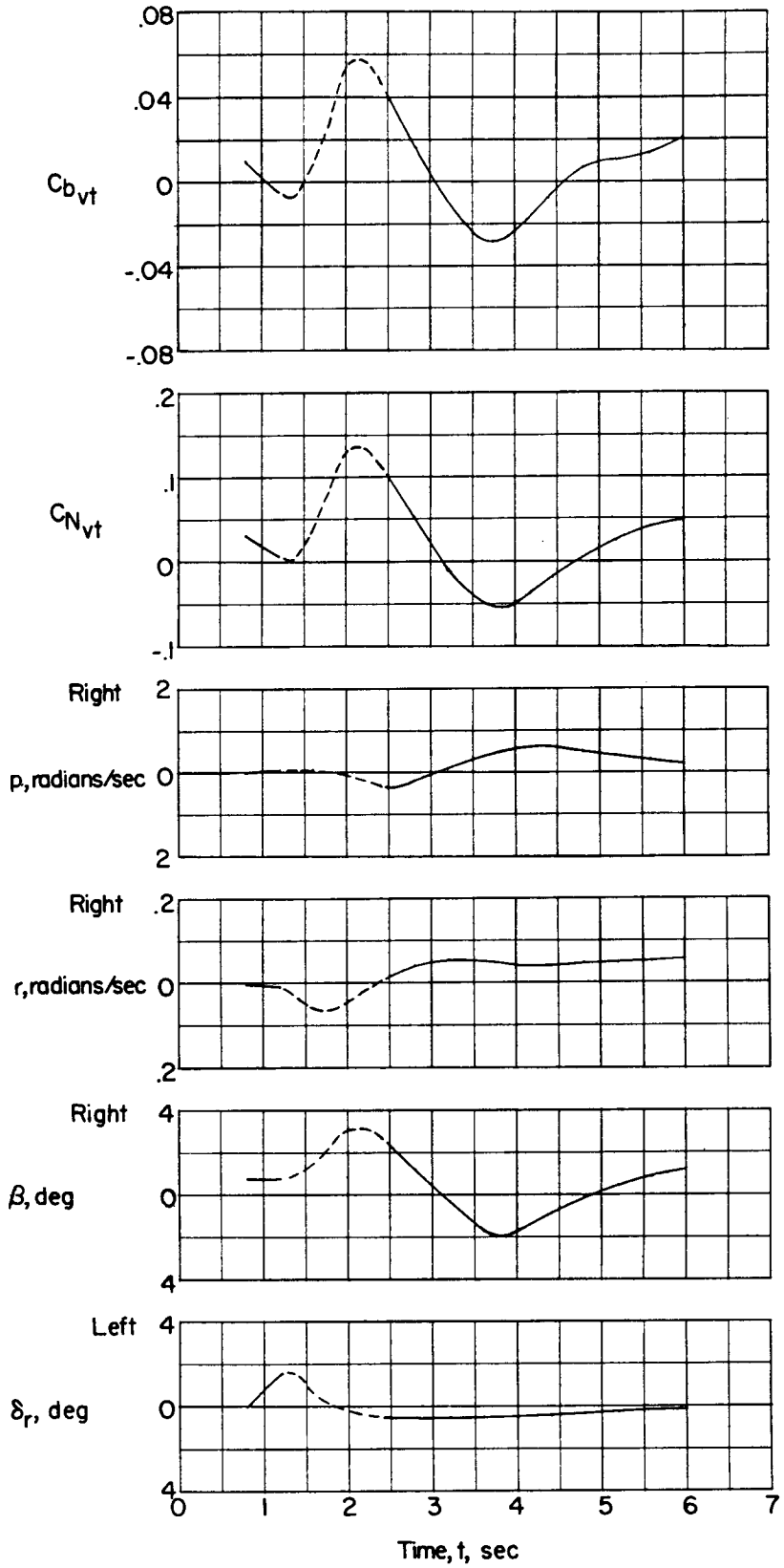

(a) M = 0.52; h_p = 23,000 feet.

Figure 3.- Time histories of airplane motions and vertical tail loads resulting from typical rudder pulse maneuvers at several Mach numbers.

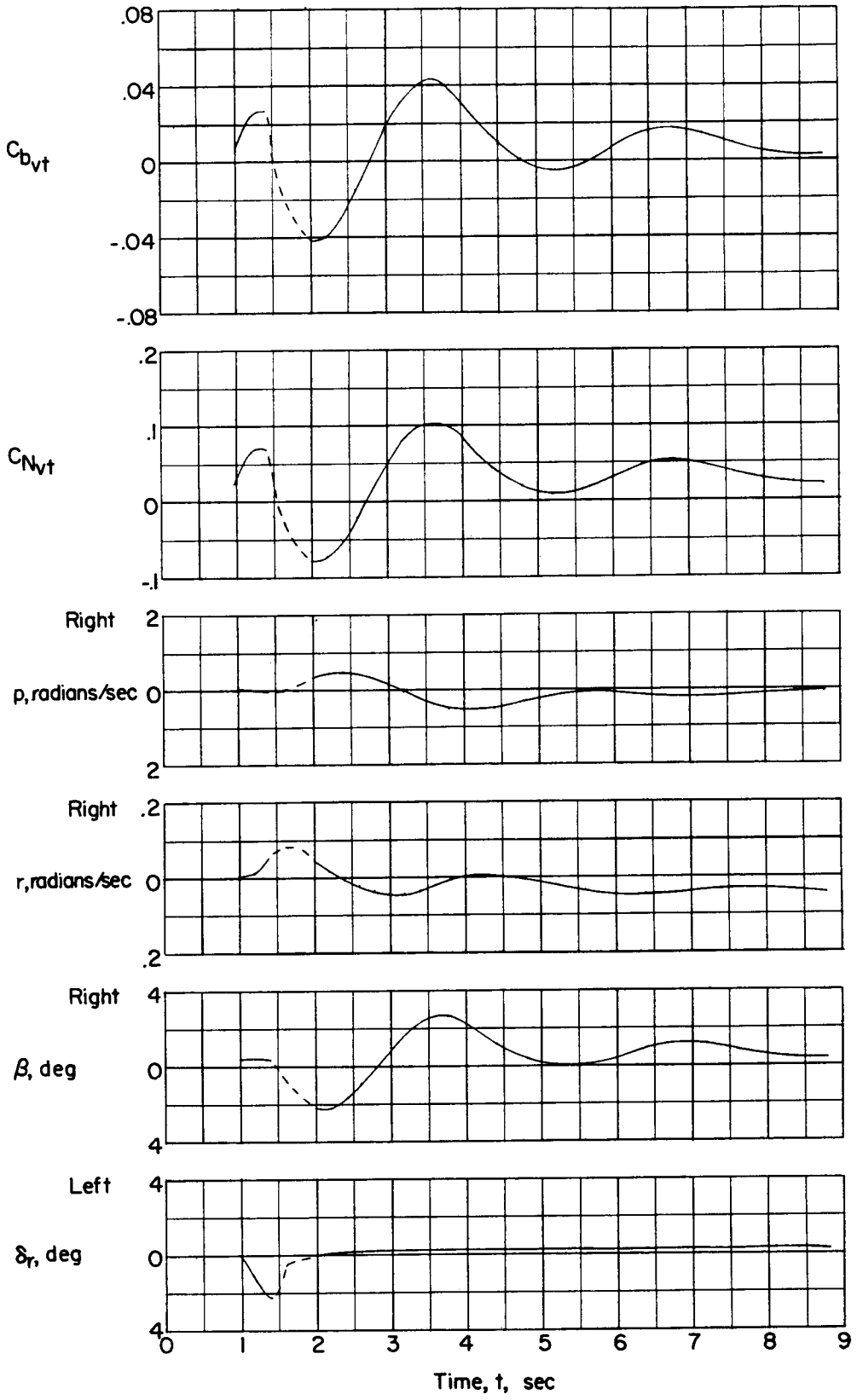

(b) M = 0.71; h_p = 31,000 feet.

Figure 3.- Continued.

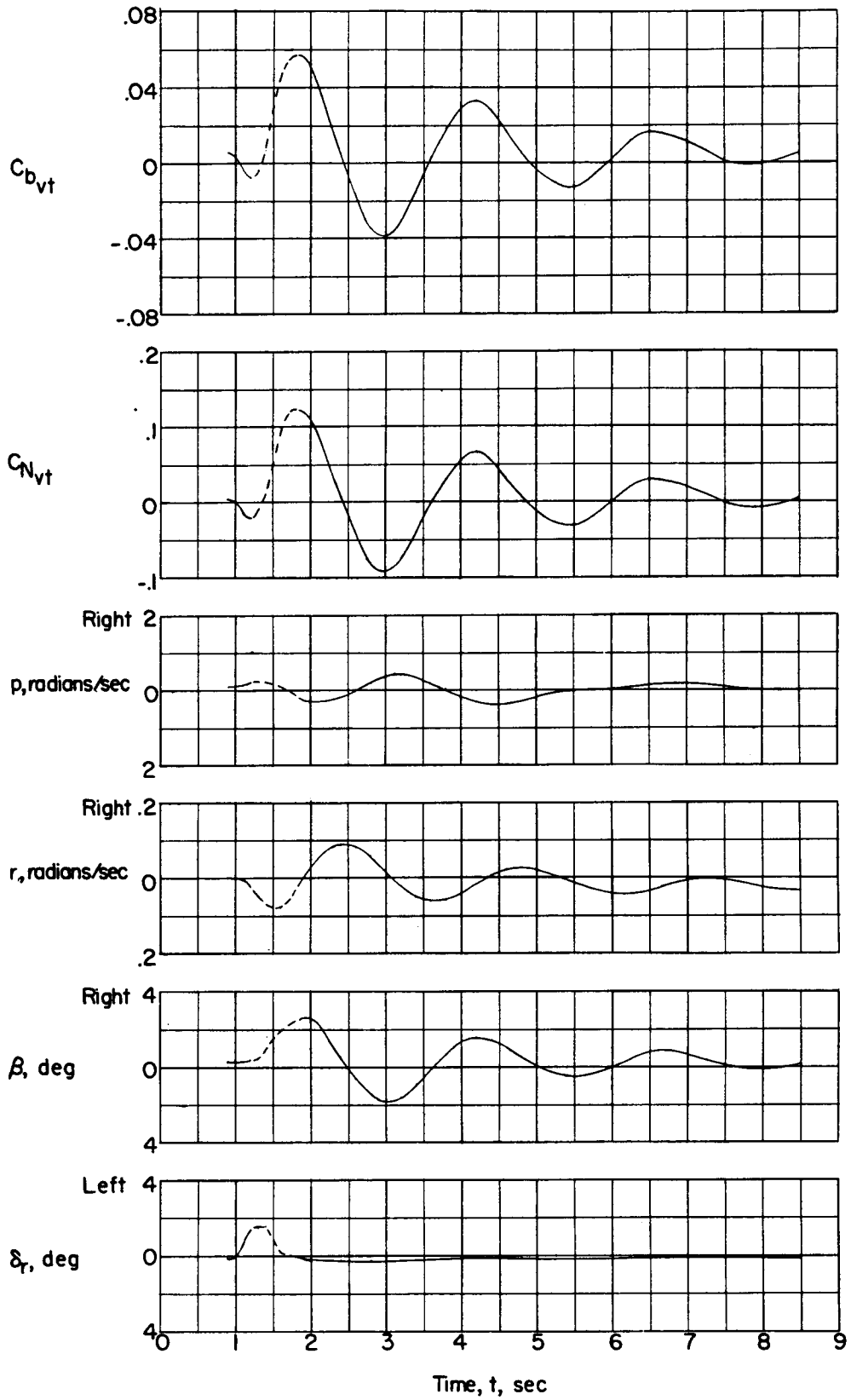

(c) M = 0.87; h_p = 30,000 feet.

Figure 3.- Concluded.

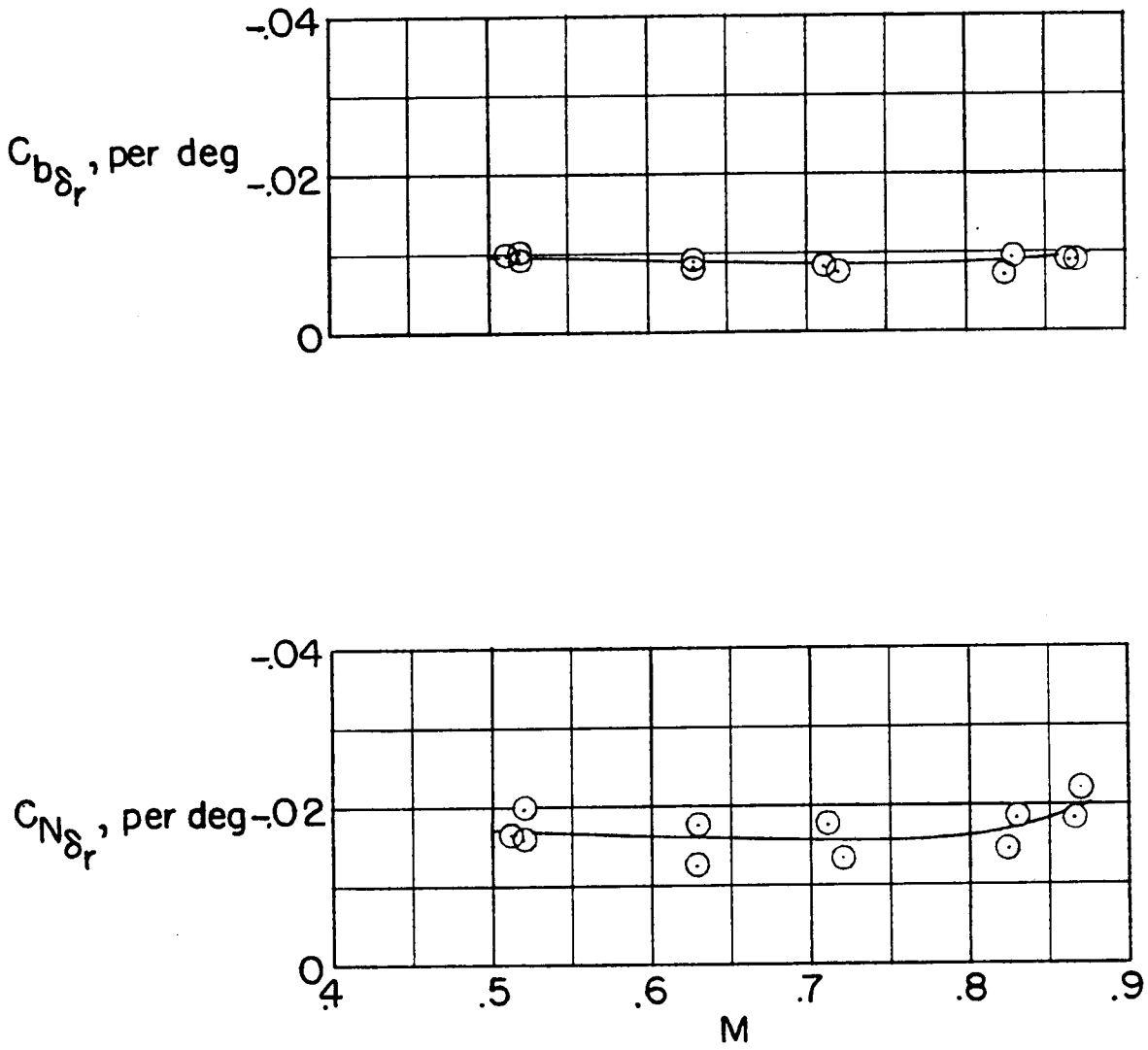

Figure 4.- Variation with Mach number of vertical-tail bending-moment and normal-force coefficients caused by rudder deflection.

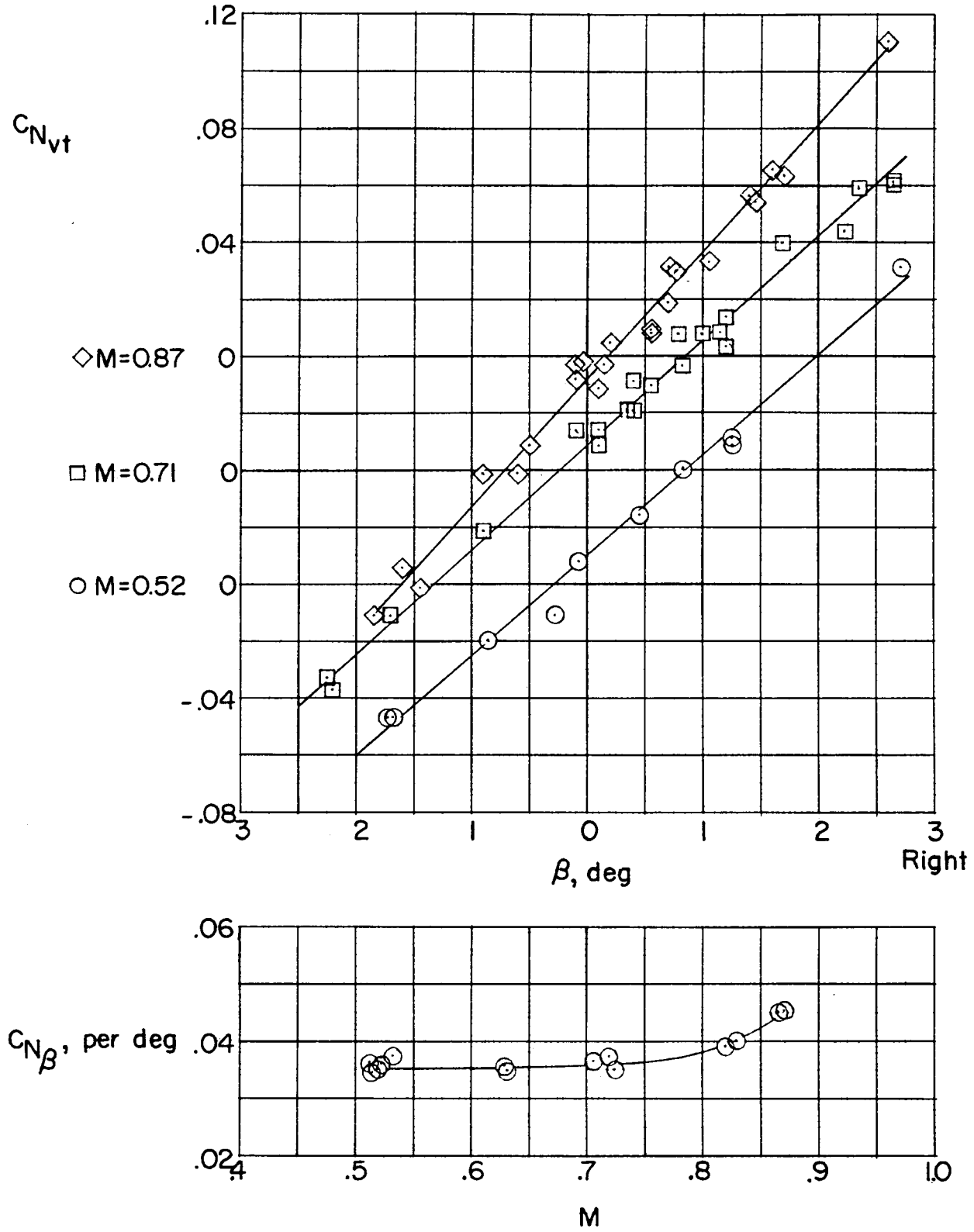

Figure 5.- Variation of vertical-tail normal-force coefficient with sideslip angle, and the normal-force curve slope variation with Mach number during rudder-fixed oscillations.

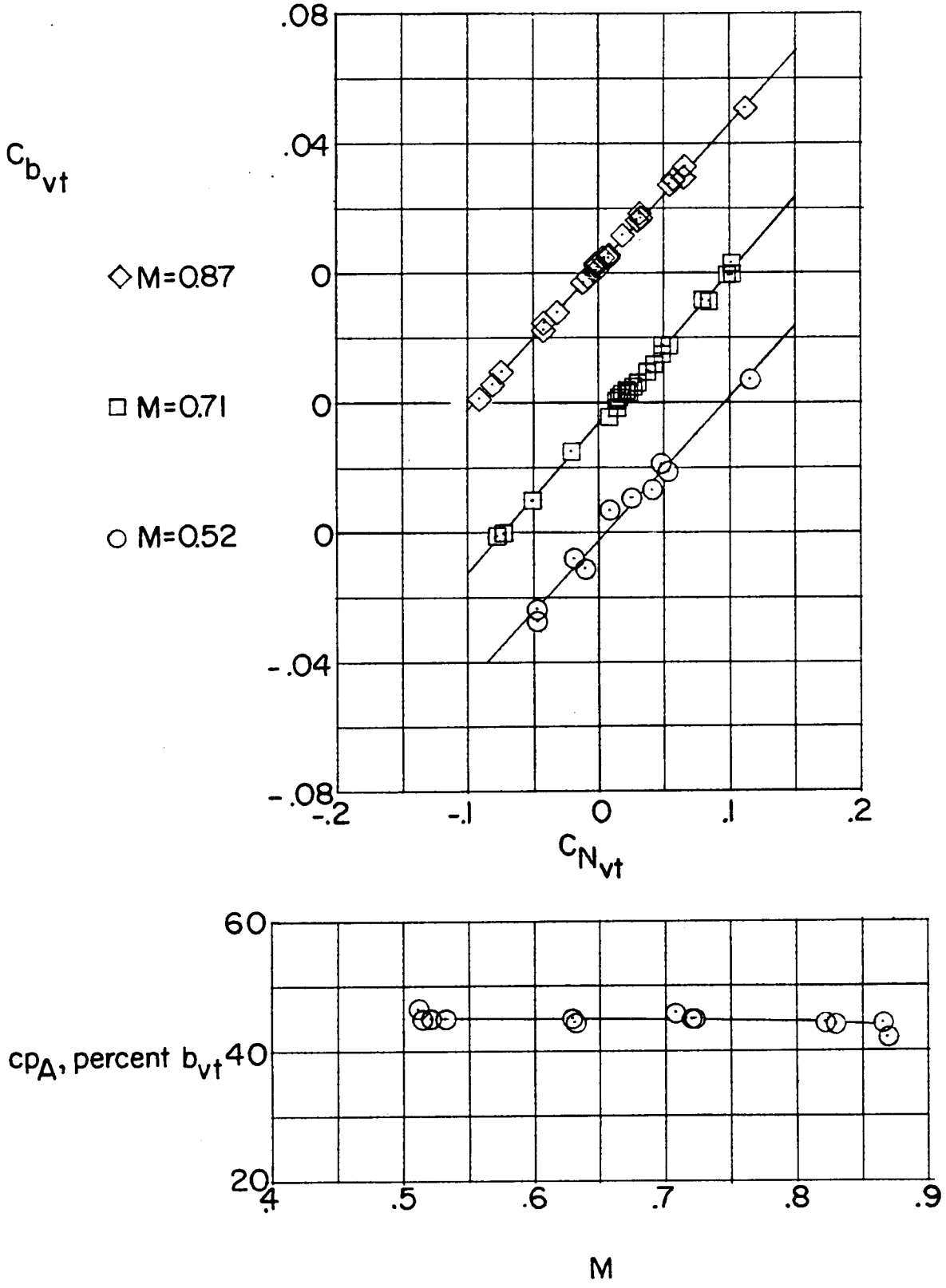

Figure 6.- Variation of vertical-tail bending-moment coefficient with normal-force coefficient and the variation with Mach number of the center of pressure of the additional air load during rudder-fixed oscillations.

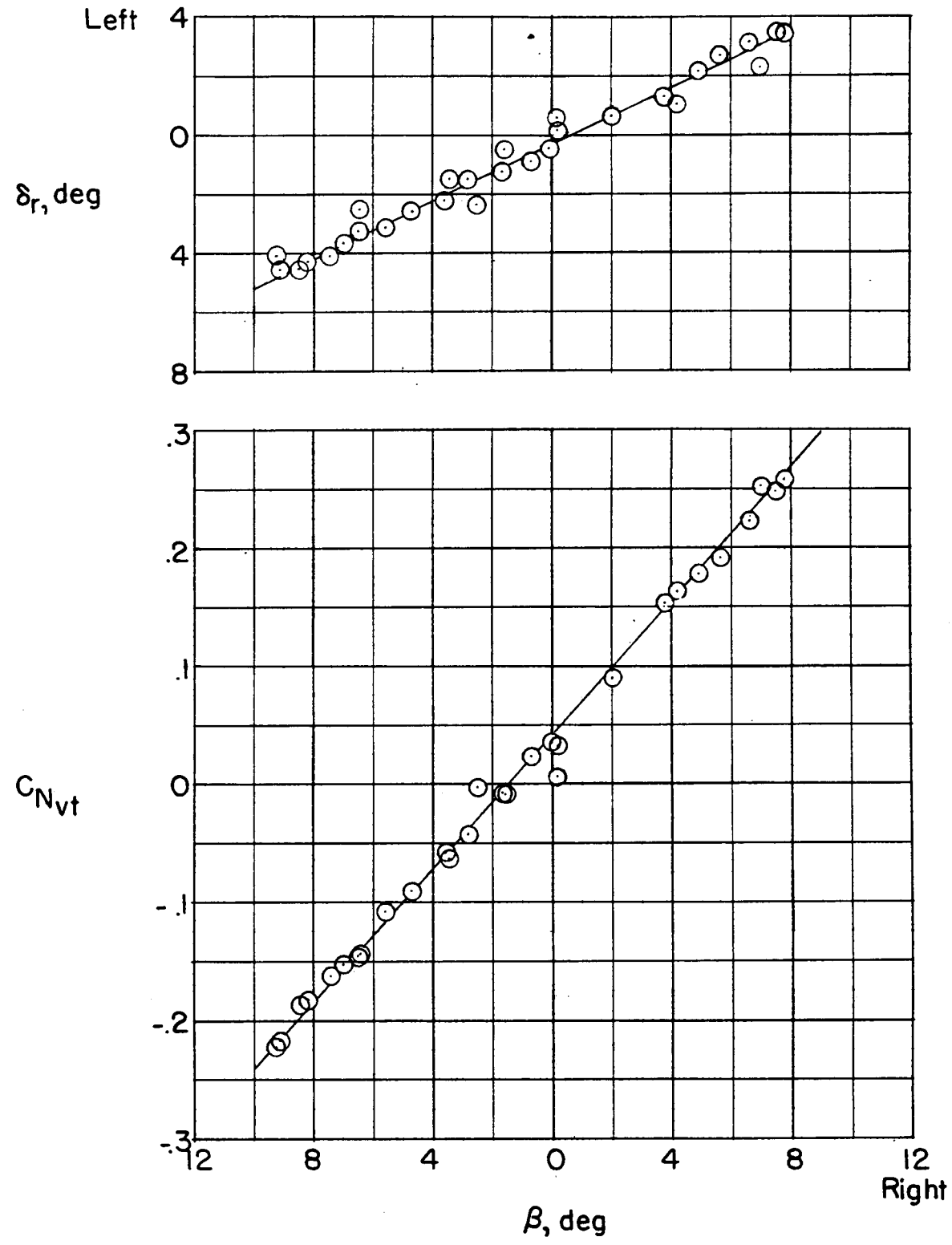

(a) M = 0.52; h_p = 29,000 feet.

Figure 7.- Variation of rudder deflection and vertical-tail normal-force coefficient with sideslip angle from several representative trimmed sideslip maneuvers.

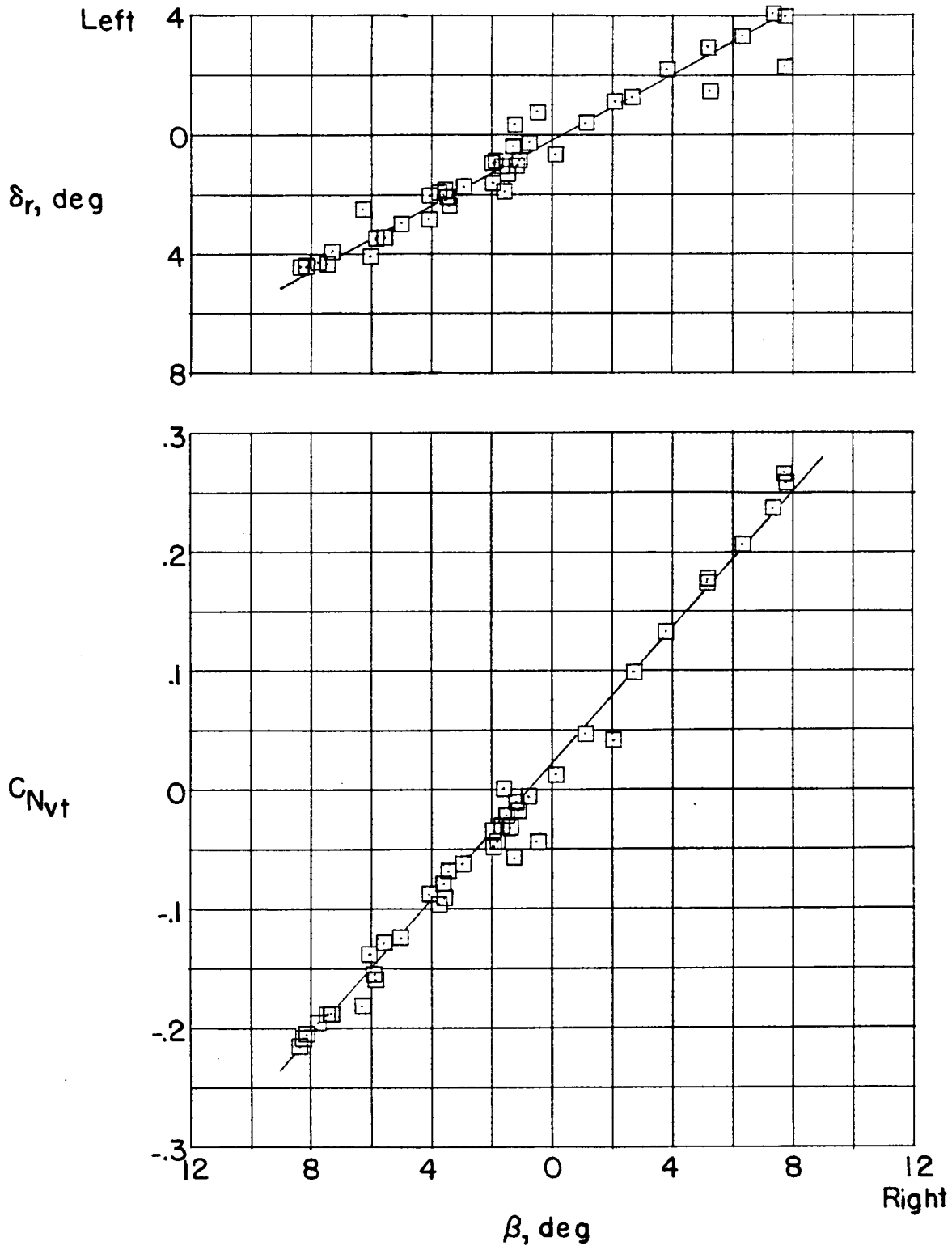

(b) M = 0.72; h_p = 30,000 feet.

Figure 7.- Continued.

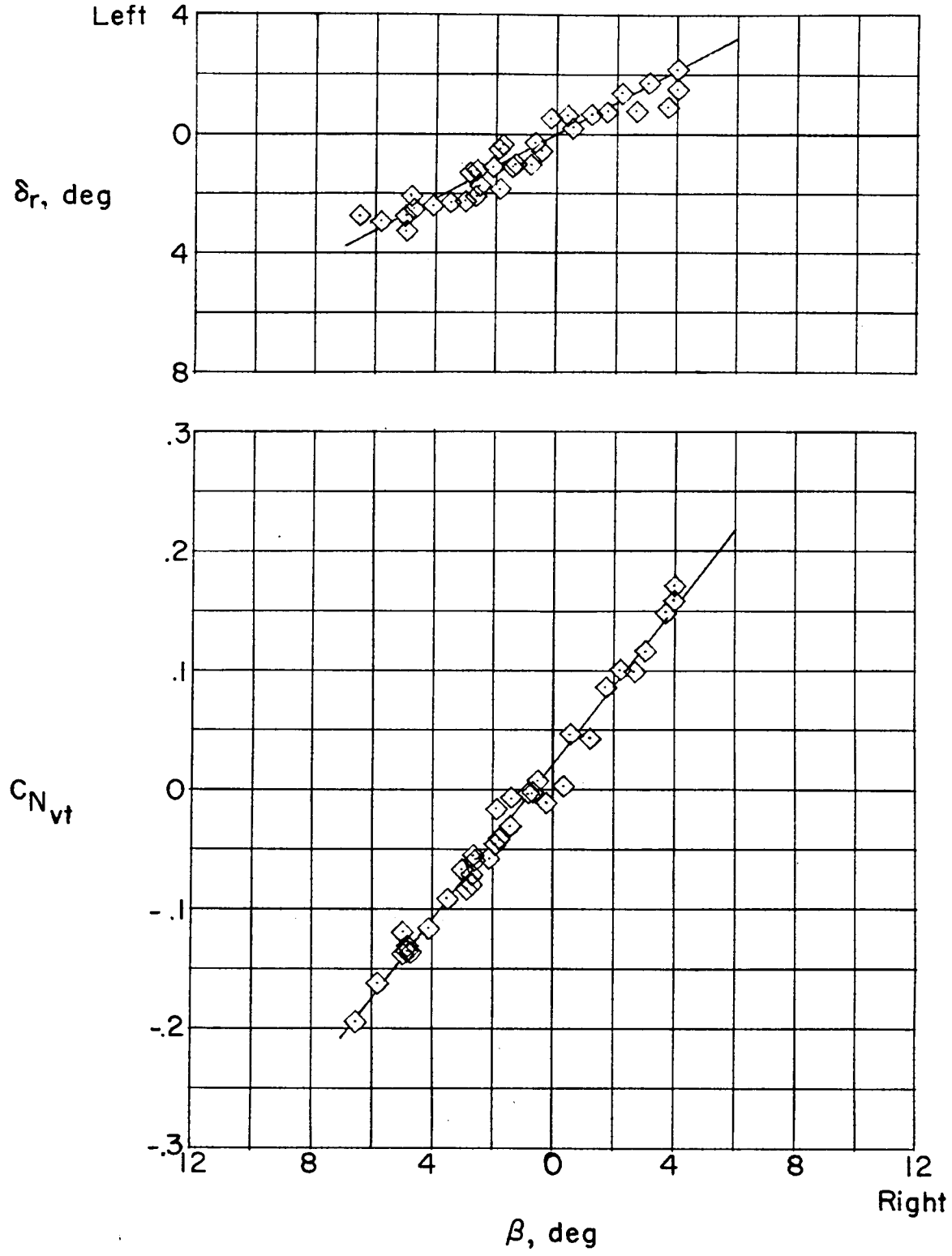

(c) M = 0.85; h_p = 22,400 feet.

Figure 7.- Concluded.

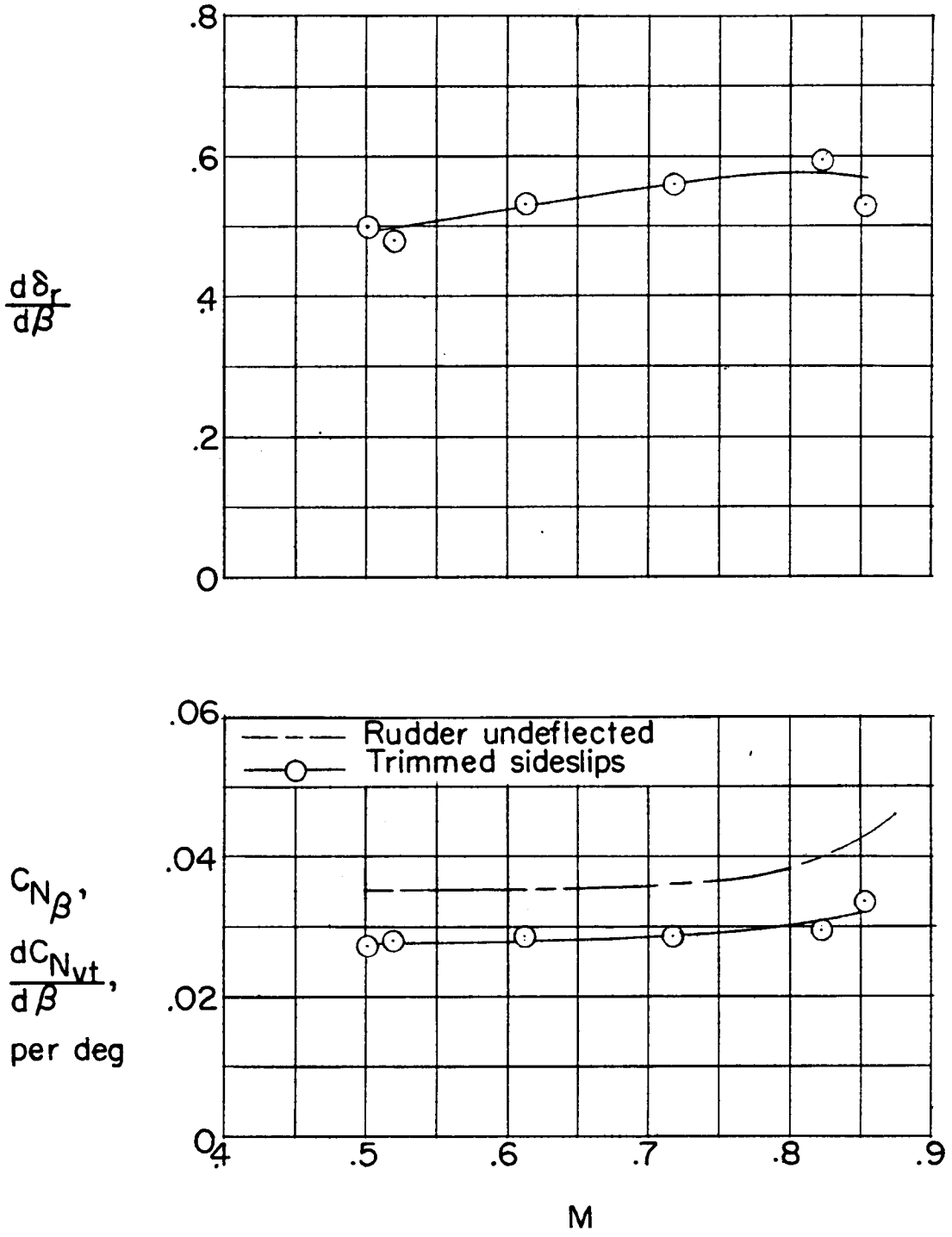

Figure 8.- Variation with Mach number of the rudder required to sideslip and the vertical-tail normal-force curve slope from trimmed sideslip maneuvers showing the effect of rudder deflection.

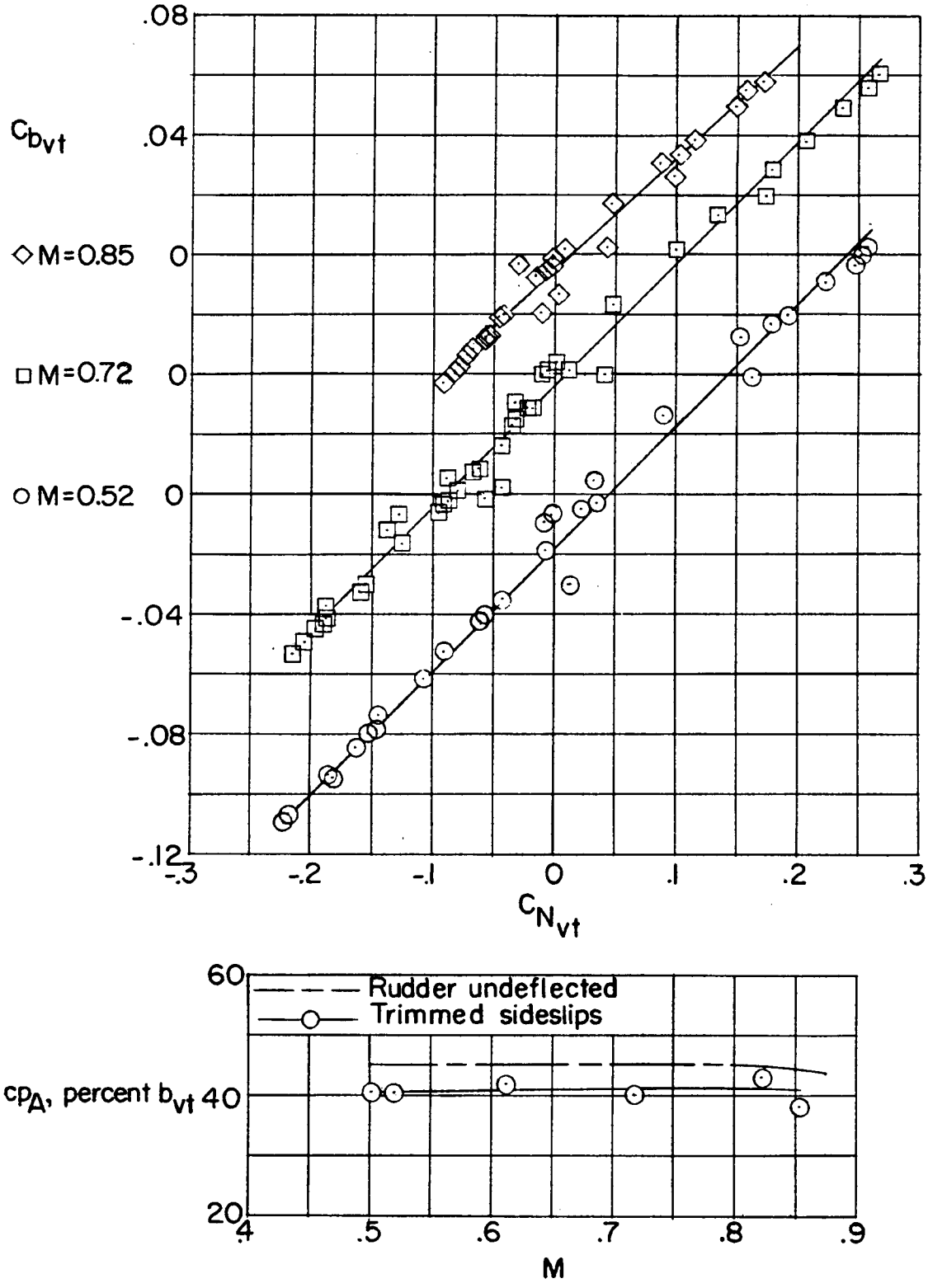

Figure 9.- Variation of vertical-tail bending-moment coefficient with normal-force coefficient during trimmed sideslips, and the variation with Mach number of the center of pressure of the additional air load showing the effect of rudder deflection.